Realization of space-dependent interactions by an optically controlled magnetic *p*-wave Feshbach resonance in degenerate Fermi gases

Guoqi Bian,[1,2] Lianghui Huang,[1,2] Donghao Li,[1,2] Zengming Meng,[1,2] Liangchao Chen,[1,2] Pengjun Wang [1,2,*] and Jing Zhang[1,†]

[1]*State Key Laboratory of Quantum Optics and Quantum Optics Devices, Institute of Opto-electronics, Shanxi University, Taiyuan, Shanxi 030006, People's Republic of China*

[2]*Collaborative Innovation Center of Extreme Optics, Shanxi University, Taiyuan, Shanxi 030006, People's Republic of China*

We report experimental realization of the space-dependent interaction by optical controlled narrow *p*-wave magnetic Feshbach resonance in a ^{40}K Fermi gas. A space varied optical field at the tune-out wavelength is applied to illuminate the atomic sample, which drives the bound-to-bound molecular transition to shift the energy of a closed-channel molecule state. Due to the position varied atomic interaction induced by the different laser intensity distribution across the entire Fermi atom cloud, the space-dependent atomic loss rate is observed. This scheme provides a control technique to study the Fermi gas with the space-dependent atomic *p*-wave interaction, and has great potential in quantum simulation.

The spatial and temporal engineering of atomic interaction in ultracold atom gases opens routes to study numerous interesting quantum phenomena, such as the simulation of black holes in Bose-Einstein condensate (BEC) [1,2], new types of quantum liquids [3,4], long-living Bloch oscillations of gap-soliton matter waves in optical lattices [5], controlled interfaces between quantum phases [6], localized collapse of a Bose condensate [7,8], Floquet symmetry-protected topological phase [9], steady-state currents from interaction-induced transport [10], and even the application of precise magnetic field sensors based on single atom transistors [11].

Magnetic-field-induced Feshbach resonance, which occurs when the bound molecular state in a closed channel is coupled to the scattering state of two colliding atoms in an open channel, is a powerful tool to control the atomic interaction by an external magnetic field and has been widely used in studying strongly correlated quantum atomic gases [12]. Based on magnetic Feshbach resonances and magnetic field gradients, collisionally inhomogeneous condensate was studied [13–16] and realized experimentally [17].

An alternative approach is optical-field-induced Feshbach resonance, using a near photoassociation resonance laser field to couple the excited bound state to the ground scattering state, which is better suited for alkaline-earth metal atoms without magnetically insensitive electronic ground states [18,19]. In recent years the optical control of magnetic Feshbach resonance has attracted a lot of attention in experiment and theory, because the laser field has higher degree of controllability in time and spatial resolution compared to the external magnetic field [8,20–29]. Based on optically controlled magnetic Feshbach resonance, the control laser field couples the ground bound state to the excited bound state, resulting in a light shift of the ground bound state in a closed channel. Therefore, the large detunings from the free atom transitions of this control laser can suppress atom loss. Furthermore, the wavelength of the control laser can be chose at tune-out wavelength (between D1 and D2 lines) that the ac-Stark shift cancels [30–38]. Thus the control laser only generates ac-Stark shift between bound-to-bound transitions, and has no influence on the ground state of free atoms. Also, the control laser does not significantly distort the trapping potential when the laser is around the tune-out wavelength.

In this paper, we report an experiment on the space-dependent optical control of narrow *p*-wave Feshbach resonance in a degenerate Fermi gas of ^{40}K. Here, an optical field is chosen to fulfill two requirements. One is that the laser wavelength should be near the tune-out wavelength 768.9701 nm [38] to minimize the distortion of the trapping potential by minimizing the ac-Stark shift for free atoms in the ground state. The other is that the frequency should be nearly resonant with a bound-to-bound molecule state transition. The atom loss spectra are measured at different laser powers, which shows the shift of *p*-wave resonance manipulated by the optical field. We observe the space-dependent atomic loss from absorption images in time of flight (TOF), which arise from the space varied atomic interaction induced by the spatially inhomogeneous light intensity distribution.

Our experiment starts with a degenerate ^{40}K Fermi gas in the hyperfine state $|F = 9/2, m_F = 9/2\rangle$ with atom number 2×10^6 and at temperature $T \approx 300$ nK $= 0.3T_F$ in a crossed 1064 nm optical dipole trap [39] with mean trapping frequency $\varpi \simeq 2\pi \times 80$ Hz, where $T_F = \hbar\varpi(6N)^{1/3}/k_B$ is the Fermi temperature and k_B is the Boltzmann constant, as shown

*Corresponding author: pengjun_wang@sxu.edu.cn
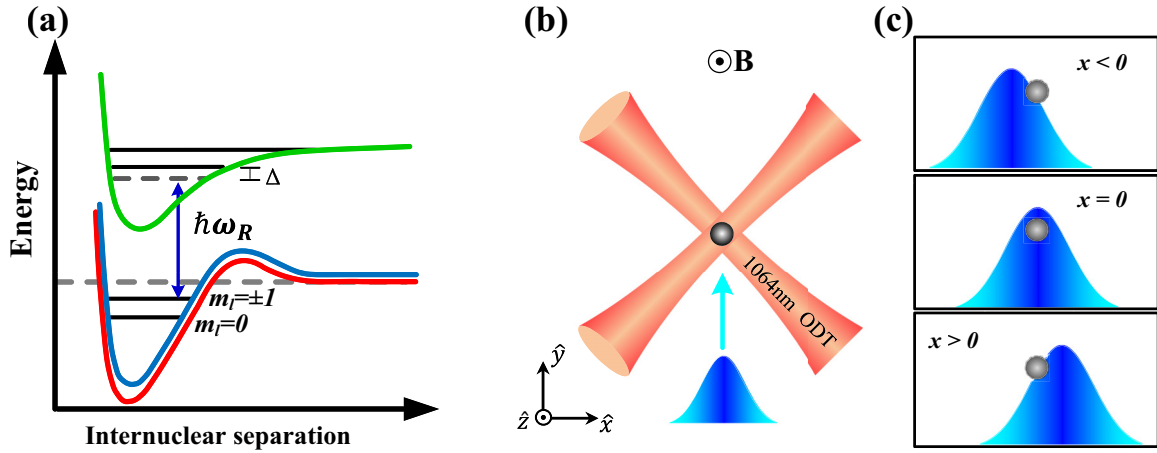†Corresponding author: jzhang74@yahoo.com; jzhang74@sxu.edu.cn

FIG. 1. (a) Energy diagram of two atoms for optical control of *p*-wave Feshbach resonance. A single control laser field with frequency ω_R (detuning Δ) is applied to drive the transition from a ground bound molecular state in the closed channel to an excited bound molecular state. (b) Schematic diagram of the experimental setup. The ^{40}K Fermi gas is trapped in an optical dipole trap composed of the two 1064 nm crossed beams in a homogeneous magnetic field $B_{exp}\hat{z}$. A single control laser beam with linear polarization in the $\hat{z}$ direction is propagating along the $\hat{y}$ direction. (c) The displacement between the single control laser beam and the atomic cloud is adjusted. The single control laser beam has a larger waist compared to the size of the trapped Fermi gas. The blue area is the intensity profile of the single control Gaussian beam.

in Fig. 1(b). The Thomas-Fermi radius of the trapped atom cloud is 78 μm. For the investigation of *p*-wave Feshbach resonance in $|9/2, -7/2\rangle$, the fermionic atoms are first transferred to the $|9/2, -9/2\rangle$ state via a rapid adiabatic passage induced by a radio frequency (rf) field at $B = 5$ G. Then, the Fermi gas is transferred to the $|9/2, -7/2\rangle$ state using a rf field with duration of 30 ms at a external magnetic field of 219.4 G. After this process, the external homogeneous magnetic field is ramped to the final value close the Feshbach resonance B_0. A linearly polarized control laser beam with $1/e^2$ radii of 200 μm is used to illuminate the atom cloud along the *y* direction. After the atomic ensemble is held for a certain time, the magnetic field, the control laser beam, and the optical dipole trap are simultaneously switched off; the absorption imaging of remaining atoms is performed after a time of flight (TOF) of 15 ms, to measure the atom loss spectra.

In order to realize the space-dependent scattering length in the size of the atomic cloud, we employ a narrow *p*-wave Feshbach resonance of the $|F = 9/2, m_F = -7/2\rangle$ state at $B \sim 198$ G (the $m = 0$ resonance occurs at 198.8 G and the $m = \pm 1$ resonance at 198.3 G). This increases the sensitivity of scattering length to the gradient light shift induced by the control laser field on the length scale of micrometers, and so we easily observe the local atom losses in the density profile of the Fermi atoms. The control laser beam generated from a Ti:sapphire laser is linearly polarized along $\hat{z}$ with $1/e^2$ radius of 200 μm, which is larger compared to the Thomas-Fermi radius of the Fermi gas, and illuminates the atom cloud along the *y* direction. Because the frequency of the laser is tuned to the vicinity of the tune-out wavelength $\lambda_{to} = 768.9701$ nm (389.862 THz), and the ac-Stark shift of the laser is only $2\pi \times 2$ kHz, while the ac-Stark shift of the dipole trap is up to $2\pi \times 0.34$ MHz, and the power is 270 mW with a waist of 40 μm. Therefore, the control laser approaches zero energy shift for free atoms and induces little spontaneous scattering compared with the ac shift of the dipole trap.

We first measure the bound-to-bound transitions for excited ^{40}K$_2$ molecules below the $^2P_{3/2} + {}^2S_{1/2}$ threshold by applying a single control laser field ω_L to illuminate the atom cloud near the *p*-wave Feshbach resonance of $|9/2, -7/2\rangle \otimes |9/2, -7/2\rangle$ in the magnetic field $B = 198.3$ G. In our previous work, the bound-to-bound transitions for excited ^{40}K$_2$ molecules were measured below the $^2P_{1/2} + {}^2S_{1/2}$ threshold (the laser frequency is a red-detuning of the D1 line). Here, the laser frequency is scanned between D1 and D2 lines (770.1 to 766.7 nm). Figure 2 shows the atom loss spectra after the single control laser beam near the *p*-wave Feshbach resonance of $|9/2, -7/2\rangle \otimes |9/2, -7/2\rangle$. The atomic cloud locates at the center of the control laser profile with the power about 60 mW. Here, the magnetic field is fixed on the $m = \pm 1$ resonance at 198.3 G. When the laser is far detuned from the bound-to-bound molecular transitions (it can be regarded as the case of no light), the atoms are located at the exact Feshbach resonance and so are subject to inelastic loss since the energy of the closed-channel molecular state $m = \pm 1$ coincides with the energy of two free atoms. When the laser field is tuned near the resonance on the bound-bound molecular transition, the laser shifts the Feshbach resonance position via the ac-Stark effect, which suppresses the loss caused by the underlying resonance. Such suppression in Fig. 2, which corresponds to a bound-to-bound transition from the ground to the excited state ^{40}K$_2$ molecules, shows up as a peak in the loss spectrum. Here, we would like to emphasize that the generation of the peak has nothing to do with the molecular excitation losses, and the width of the peak depends on the coupling strength of the control laser, which is not related to the linewidth of the excited molecular state.

We obtain the six strong bound-to-bound molecular transitions near the tune-out wavelength when the frequency of the control laser is scanned with the step of $2\pi \times 1$ GHz. A specific molecular transition at $\omega_L \sim 2\pi \times 389.881$ THz is closest to the tune-out wavelength for ^{40}K and is highlighted
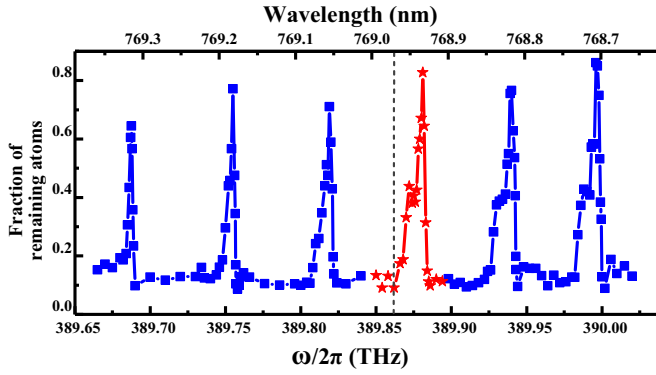
FIG. 2. Bound-to-bound spectroscopy below the $^2P_{3/2} + ^2S_{1/2}$ threshold near the p-wave Feshbach resonance of $|9/2, -7/2\rangle \otimes |9/2, -7/2\rangle$ at the magnetic field $B = 198.3$ G. The peaks are created because the control laser shifts the Feshbach resonance position by the ac-Stark effect and reduces the atomic loss (protects atoms). The duration of laser pulse is 8 ms, and the power of the laser is 60 mW. A molecular transition at $\omega_L \sim 2\pi \times 389.881$ THz used in the experiment is highlighted with red stars, and the tune-out wavelength for ^{40}K atoms is marked by a vertical dashed line. The linewidth of the bound-to-bound spectroscopy is around $2\pi \times 10$ GHz. Here, the power of the control laser is chosen as $\Omega(0) = 2\pi \times 64.72$ kHz $\times \sqrt{I(0)/(\text{mW/cm}^2)} \approx 2\pi \times 20$ MHz. "Fraction of remaining atoms" means the ratio between the number of remaining atoms after the Feshbach interaction and the number of initial atoms.

in Fig. 2 with red stars; it is used in our experiment to study the space-dependent atomic interaction. The control laser closest to the tune-out wavelength causes zero energy shift on the free atoms and does not create any parasitic dipole force, and still allows us to see the spatial control of interactions.

Next we study the optically controlled magnetic p-wave Feshbach resonance by applying the control laser beam with red detuning $\Delta_L = 2\pi \times (-6)$ GHz to the bound-to-bound transition $\omega_L \sim 2\pi \times 389.881$ THz. When the control laser illuminates the Fermi gas, the energy of the closed-channel bound state is effectively shifted due to the coupling to the excited molecular state. We compare the atomic loss spectra as a function of the magnetic field for different intensities of the control laser field, as shown in Fig. 3. Due to the red detuning for the bound-to-bound transition, the ac-Stark shift can bring the molecular state far away from the atomic state in the incoming channel, and therefore it requires more Zeeman energy at higher magnetic field to bring the free atomic scattering threshold close to the molecule energy level. In other words, the peaks of the bound-to-bound spectroscopy in Fig. 2 are created because the control laser shifts the Feshbach resonance position by the ac-Stark effect and reduces the atomic loss (protects atoms). Therefore, the shifts observed in Fig. 3 are consistent with the linewidths of the bound-to-bound spectroscopy observed in Fig. 2. We can clearly see that the p-wave Feshbach resonance is shifted to the high magnetic field. The optical control of different components of the p-wave Feshbach resonance ($m = \pm 1, 0$) has been described in detail in our previous work [28]. The shift of the Feshbach resonance position can be expressed by an equation derived
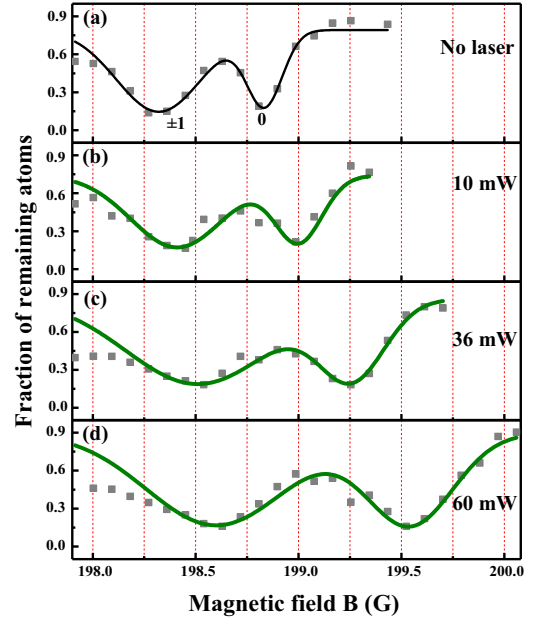

FIG. 3. The optical control of the p-wave Feshbach resonance by a single laser beam with red detuning. (a) Atom loss spectra of the p-wave Feshbach resonance of $|9/2, -7/2\rangle \otimes |9/2, -7/2\rangle$ without optical control. The left loss dip is located at 198.3 G, arising from the coupling between the atomic state of free atoms and the molecular state $m = \pm 1$ in the closed channel, and the right loss dip is located at 198.8 G for $m = 0$. Atom loss spectra of the shifted p-wave Feshbach resonance by a single control laser field with powers 10 mW (b), 36 mW (c), and 60 mW (d). Here, the detuning of the control laser is $\Delta_L = 2\pi \times (-6)$ GHz. The magnetic shift value of the $m = \pm 1$ resonance is around 0.35 Gauss in (d) compared to without control laser in (a). The solid green curves are Lorentzian fits to extract the resonance parameters.

from a microscopic coupled-channel model [28,40,41],

$$\delta\mu(B_s(r) - B_0) = -\text{Re}\left[\frac{\Omega^2(r)}{\Delta_L - i\gamma/2}\right], \quad (1)$$

where B_s and B_0 are the magnetic field position for resonances in the presence and in the absence of the optical field, $\delta\mu$ ($0.134\mu_B = 2\pi \times 0.18755$ MHz/G) is the magnetic moment difference between the closed and open channels [12], Δ_L is the laser detuning from the excited molecular states, and γ is the spontaneous-emission rate of excited molecular states. $\Omega(r) \propto \sqrt{I(r)}$ represents the laser induced coupling between the closed-channel molecule and the excited molecular state. From the loss spectra shown in Fig. 3 and Eq. (1), we understand that the different shifts of Feshbach resonance position can be induced by the different driving laser powers. Subsequently, we obtain that the coupling strength is around $2\pi \times 64.72$ kHz $\times \sqrt{I(0)/(\text{mW/cm}^2)}$ and γ is about $2\pi \times 6$ MHz.

In the following we study the space-dependent interaction by optically controlled magnetic Feshbach resonance. The displacement between the atom cloud and the control laser field determines the different laser intensity slopes $I(x)$ across the atom sample, which will induce the space-dependent interaction. Figures 4(a), 4(b), and 4(c) show TOF images (15 ms) of the Fermi atoms and the integrated density profile along
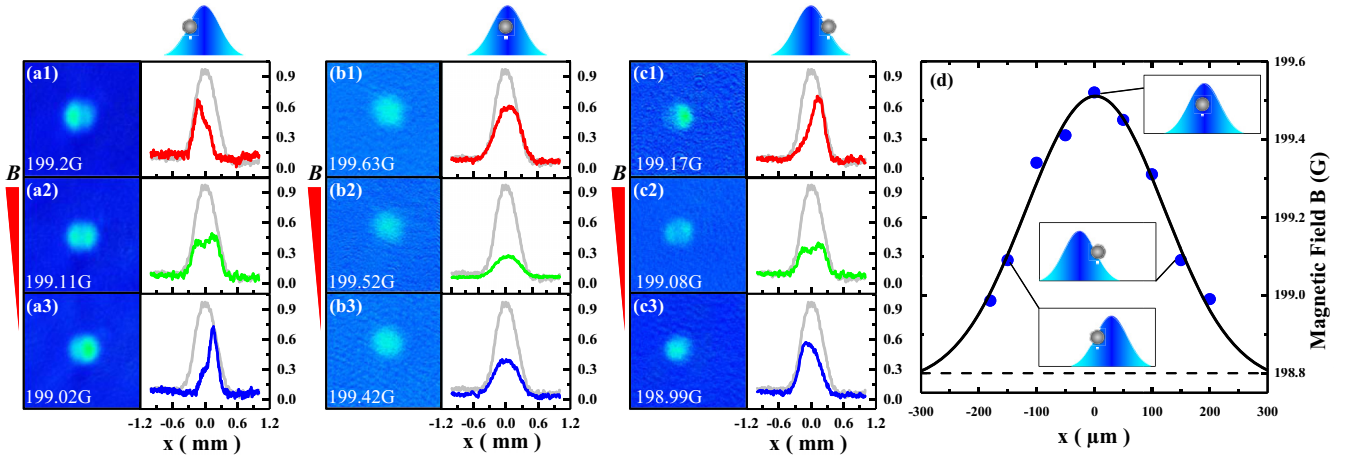
FIG. 4. (a), (b), and (c) are the TOF images of the atom cloud and the corresponding integrated density profile along the x direction at different external magnetic fields in the cases of (a) $\Delta x = -150\ \mu$m, (b) $\Delta x = 0\ \mu$m, and (c) $\Delta x = 150\ \mu$m. Here, a single control laser with power 60 mW, detuning $2\pi \times (-6)$ GHz, and duration 5 ms is applied. The gray curves in (a), (b), and (c) are the integrated density profiles of the Fermi gas without the control laser. (d) The shifted position of the p-wave Feshbach resonance of $m = 0$ as a function of the displacement between the center of the laser beam and the atomic cloud. The dark solid line is only to guide the eye.

the y direction for the different external magnetic fields and displacements between the atom cloud and the control laser field. We observe large local loss in the degenerate Fermi gases. Note that reaching quantum degenerate of Fermi gases is important to observe the local loss in the atomic sample. The timescale for the spatial distribution going over to the momentum distribution is longer for a degenerate gas than for a thermal gas. Here, a control laser beam with power 60 mW and detuning $2\pi \times (-6)$ GHz is applied. The external magnetic field is scanned near the position of the p-wave Feshbach resonance of $m = 0$.

For the case of displacement $\Delta x = -150\ \mu$m, when changing the external magnetic field from high to low values, the local loss region is moved from the right part to the left part, as shown in Figs. 4(a1)–4(a3). This is because the right part of the atomic sample feels the stronger control laser and so its Feshbach resonance position locates in the higher magnetic field. When the largest local loss locates at the center of the atomic cloud [see Fig. 4(a2)], it indicates that the center part of the Fermi cloud experiences strong

interaction with the diverged scattering length and the positive and negative scattering lengths at the two sides. As a comparison, for the case of displacement $\Delta x = 150\ \mu$m, the large local loss region is moved from the left part to the right part (the opposite direction) when changing the external magnetic field from high to low values (same as above), as shown in Figs. 4(c1)–4(c3). For the case of $\Delta x = 0\ \mu$m, the atomic sample feels an almost homogeneous control laser, which induces the uniform atom losses in the entire atom cloud. At the same time, the largest shift of the Feshbach resonance to high magnetic field is obtained for this case. At last, we can give the $m = 0$ p-wave Feshbach resonance position as a function of the displacement between the laser and Fermi gas cloud, as shown in Fig. 4(d). Here, we label the external magnetic field as the Feshbach resonance position when the largest local loss locates at the center of the atomic cloud. Therefore, the shift of the p-wave Feshbach resonance matches the Gaussian intensity distribution of the control laser.

We observe the space-dependent atomic loss from the absorption images with time of flight (TOF), which arises from
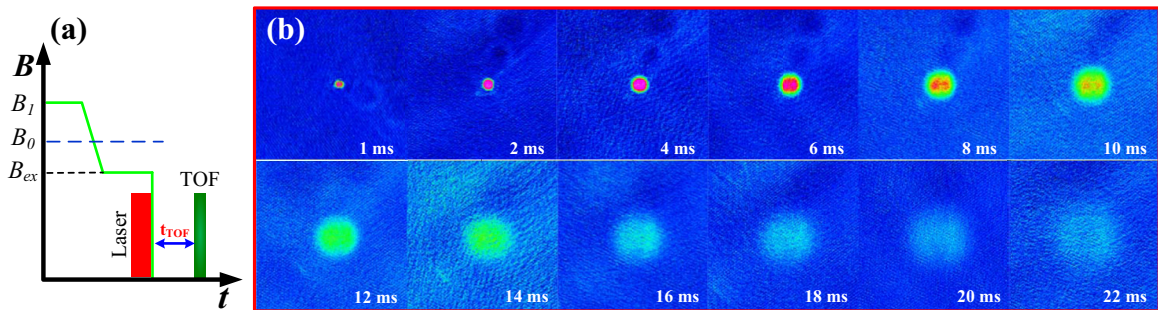

FIG. 5. Evolution of the atomic density as a function of the different TOF t_{TOF}. (a) Time sequence of the homogeneous bias magnetic field, the control laser, where $B_1 = 219$ G and $B_{ex} = 199.11$ G are the initial and final external magnetic fields, respectively, and $B_0 \approx 198.3$ G is the Feshbach resonant point. (b) The TOF images of the atomic cloud for the different TOF t_{TOF}. Here, a single control laser with power 60 mW, detuning $2\pi \times (-6)$ GHz, and duration 5 ms is applied. The displacement is $\Delta x = -150\ \mu$m and the final external magnetic field is $B_{ex} = 199.11$ G.
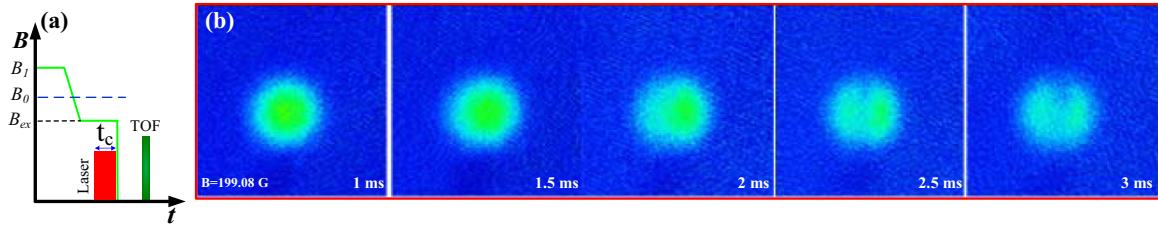
FIG. 6. Evolution of the atomic density as a function of the pulse duration time of the control laser beam. (a) Time sequence of the homogeneous bias magnetic field, the control laser. (b) The TOF images (15 ms) of the atomic cloud for the different duration times t_c of the control laser. Here, the displacement is $\Delta x = -150\ \mu$m.

the space varied atomic interaction induced by the spatially inhomogeneous light intensity distribution. Usually the atomic density distribution from TOF absorption images gives information on the momentum distribution. Here, we study the space-dependent atomic loss from the absorption images at the different TOF as shown in Fig. 5. Since the Fermi gases reach a quantum degenerate state, we can clearly see the local losses at the different TOF. Furthermore, we study the atomic loss rate by changing the pulse duration time of the control laser beam, as shown in Fig. 6. When the duration time of the control laser is larger than 3 ms, the apparent space-dependent atomic loss appears in the atomic density distribution.

In conclusion, we have demonstrated that the space-dependent interaction by optical control of a narrow *p*-wave Feshbach resonance in an ultracold Fermi gas of ^{40}K. A special optical field with frequency close to the tune-out wavelength is applied to drive the ground molecular state to an excited molecular state transition and induce ac-Stark shift of the closed channel. Employing a single control laser beam with a larger waist compared to the size of the atom cloud, the steep slope of the Gaussian profile of the laser beam can generate the space-dependent interaction. By adjusting the displacement between the control laser beam and the atom cloud, we observe the space-dependent atomic loss from the absorption images, demonstrating the space-dependent atomic *p*-wave interaction. Our scheme provides us a powerful technique to study many-body physics with *p*-wave Feshbach resonance [42–45].

[1] L. J. Garay, J. R. Anglin, J. I. Cirac, and P. Zoller, Sonic Analog of Gravitational Black Holes in Bose-Einstein Condensates, Phys. Rev. Lett. **85**, 4643 (2000).

[2] I. Carusotto, S. Fagnocchi, A. Recati, R. Balbinot, and A. Fabbri, Numerical observation of hawking radiation from acoustic black holes in atomic Bose–Einstein condensates, New J. Phys. **10**, 103001 (2008).

[3] F. Kh. Abdullaev, J. G. Caputo, R. A. Kraenkel, and B. A. Malomed, Controlling collapse in Bose-Einstein condensates by temporal modulation of the scattering length, Phys. Rev. A **67**, 013605 (2003).

[4] H. Saito and M. Ueda, Bose-Einstein droplet in free space, Phys. Rev. A **70**, 053610 (2004).

[5] M. Salerno, V. V. Konotop, and Yu. V. Bludov, Long-Living Bloch Oscillations of Matter Waves in Periodic Potentials, Phys. Rev. Lett. **101**, 030405 (2008).

[6] M. J. Hartmann and M. B. Plenio, Migration of Bosonic Particles across a Mott Insulator to a Superfluid Phase Interface, Phys. Rev. Lett. **100**, 070602 (2008).

[7] G. Dong, B. Hu, and W. Lu, Ground-state properties of a Bose-Einstein condensate tuned by a far-off-resonant optical field, Phys. Rev. A **74**, 063601 (2006).

[8] L. W. Clark, L.-C. Ha, C.-Y. Xu, and C. Chin, Quantum Dynamics with Spatiotemporal Control of Interactions in a Stable Bose-Einstein Condensate, Phys. Rev. Lett. **115**, 155301 (2015).

[9] I.-D. Potirniche, A. C. Potter, M. Schleier-Smith, A. Vishwanath, and N. Y. Yao, Floquet Symmetry-Protected Topological Phases in Cold-Atom Systems, Phys. Rev. Lett. **119**, 123601 (2017).

[10] C.-Y. Lai and C.-C. Chien, Quantification of the memory effect of steady-state currents from interaction-induced transport in quantum systems, Phys. Rev. A **96**, 033628 (2017).

[11] K. Jachymski, T. Wasak, Z. Idziaszek, P. S. Julienne, A. Negretti, and T. Calarco, Single-Atom Transistor as a Precise Magnetic Field Sensor, Phys. Rev. Lett. **120**, 013401 (2018).

[12] C. Chin, R. Grimm, P. Julienne, and E. Tiesinga, Feshbach resonances in ultracold gases, Rev. Mod. Phys. **82**, 1225 (2010).

[13] G. Theocharis, P. Schmelcher, P. G. Kevrekidis, and D. J. Frantzeskakis, Matter-wave solitons of collisionally inhomogeneous condensates, Phys. Rev. A **72**, 033614 (2005).

[14] G. Theocharis, P. Schmelcher, P. G. Kevrekidis, and D. J. Frantzeskakis, Dynamical trapping and transmission of matter-wave solitons in a collisionally inhomogeneous environment, Phys. Rev. A **74**, 053614 (2006).

[15] P. Niarchou, G. Theocharis, P. G. Kevrekidis, P. Schmelcher, and D. J. Frantzeskakis, Soliton oscillations in collisionally in-

homogeneous attractive Bose-Einstein condensates, Phys. Rev. A **76**, 023615 (2007).

[16] A. S. Rodrigues, P. G. Kevrekidis, M. A. Porter, D. J. Frantzeskakis, P. Schmelcher, and A. R. Bishop, Matter-wave solitons with a periodic, piecewise-constant scattering length, Phys. Rev. A **78**, 013611 (2008).

[17] A. Di Carli, G. Henderson, S. Flannigan, C. D. Colquhoun, M. Mitchell, G.-L. Oppo, A. J. Daley, S. Kuhr, and E. Haller, Collisionally Inhomogeneous Bose-Einstein Condensates with a Linear Interaction Gradient, Phys. Rev. Lett. **125**, 183602 (2020).

[18] P. O. Fedichev, Yu. Kagan, G. V. Shlyapnikov, and J. T. M. Walraven, Influence of Nearly Resonant Light on the Scattering Length in Low-Temperature Atomic Gases, Phys. Rev. Lett. **77**, 2913 (1996).

[19] T. L. Nicholson, S. Blatt, B. J. Bloom, J. R. Williams, J. W. Thomsen, J. Ye, and P. S. Julienne, Optical feshbach resonances: Field-dressed theory and comparison with experiments, Phys. Rev. A **92**, 022709 (2015).

[20] D. M. Bauer, M. Lettner, C. Vo, G. Rempe, and S. Dürr, Control of a magnetic Feshbach resonance with laser light, Nat. Phys. **5**, 339 (2009).

[21] P. Zhang, P. Naidon, and M. Ueda, Independent Control of Scattering Lengths in Multicomponent Quantum Gases, Phys. Rev. Lett. **103**, 133202 (2009).

[22] H. Wu and J. E. Thomas, Optical Control of Feshbach Resonances in Fermi Gases Using Molecular Dark States, Phys. Rev. Lett. **108**, 010401 (2012).

[23] Z. Fu, P. Wang, L. Huang, Z. Meng, H. Hu, and J. Zhang, Optical control of a magnetic Feshbach resonance in an ultracold Fermi gas, Phys. Rev. A **88**, 041601(R) (2013).

[24] Y.-C. Zhang, W.-M. Liu, and H. Hu, Tuning a magnetic Feshbach resonance with spatially modulated laser light, Phys. Rev. A **90**, 052722 (2014).

[25] J. Jie and P. Zhang, Center-of-mass-momentum-dependent interaction between ultracold atoms, Phys. Rev. A **95**, 060701(R) (2017).

[26] A. Jagannathan, N. Arunkumar, J. A. Joseph, and J. E. Thomas, Optical Control of Magnetic Feshbach Resonances by Closed-Channel Electromagnetically Induced Transparency, Phys. Rev. Lett. **116**, 075301 (2016).

[27] N. Arunkumar, A. Jagannathan, and J. E. Thomas, Probing Energy-Dependent Feshbach Resonances by Optical Control, Phys. Rev. Lett. **121**, 163404 (2018).

[28] P. Peng, R. Zhang, L. Huang, D. Li, Z. Meng, P. Wang, H. Zhai, P. Zhang, and J. Zhang, Universal feature in optical control of a *p*-wave Feshbach resonance, Phys. Rev. A **97**, 012702 (2018).

[29] N. Arunkumar, A. Jagannathan, and J. E. Thomas, Designer Spatial Control of Interactions in Ultracold Gases, Phys. Rev. Lett. **122**, 040405 (2019).

[30] L. J. LeBlanc and J. H. Thywissen, Species-specific optical lattices, Phys. Rev. A **75**, 053612 (2007).

[31] B. Arora, M. S. Safronova, and C. W. Clark, Tune-out wavelengths of alkali-metal atoms and their applications, Phys. Rev. A **84**, 043401 (2011).

[32] W. F. Holmgren, R. Trubko, I. Hromada, and A. D. Cronin, Measurement of a Wavelength of Light for Which the Energy Shift for an Atom Vanishes, Phys. Rev. Lett. **109**, 243004 (2012).

[33] J. Jiang, L.-Y. Tang, and J. Mitroy, Tune-out wavelengths for potassium, Phys. Rev. A **87**, 032518 (2013).

[34] Y. Cheng, J. Jiang, and J. Mitroy, Tune-out wavelengths for the alkaline-earth-metal atoms, Phys. Rev. A **88**, 022511 (2013).

[35] R. H. Leonard, A. J. Fallon, C. A. Sackett, and M. S. Safronova, High-precision measurements of the ^{87}Rb D-line tune-out wavelength, Phys. Rev. A **92**, 052501 (2015).

[36] R. Trubko, J. Greenberg, M. T. St. Germaine, M. D. Gregoire, W. F. Holmgren, I. Hromada, and A. D. Cronin, Atom Interferometer Gyroscope with Spin-Dependent Phase Shifts Induced by Light near a Tune-Out Wavelength, Phys. Rev. Lett. **114**, 140404 (2015).

[37] F. Schmidt, D. Mayer, M. Hohmann, T. Lausch, F. Kindermann, and A. Widera, Precision measurement of the ^{87}Rb tune-out wavelength in the hyperfine ground state $F = 1$ at 790 nm, Phys. Rev. A **93**, 022507 (2016).

[38] R. Trubko, M. D. Gregoire, W. F. Holmgren, and A. D. Cronin, Potassium tune-out-wavelength measurement using atom interferometry and a multipass optical cavity, Phys. Rev. A **95**, 052507 (2017).

[39] S. Chai, P. Wang, Z. Fu, L. Huang, and J. Zhang, The design of a dipole traps for Bose-Einstein condensate and degenerate Fermi gas, Acta Sin. Quantum Opt. **18**, 171 (2012).

[40] P. Zhang, P. Naidon, and M. Ueda, Scattering amplitude of ultracold atoms near the *p*-wave magnetic Feshbach resonance, Phys. Rev. A **82**, 062712 (2010).

[41] T. Köhler, K. Góral, and P. S. Julienne, Production of cold molecules via magnetically tunable Feshbach resonance, Rev. Mod. Phys. **78**, 1311 (2006).

[42] Z. Yu, J. H. Thywissen, and S. Zhang, Universal Relations for a Fermi Gas Close to a *p*-Wave Interaction Resonance, Phys. Rev. Lett. **115**, 135304 (2015).

[43] L. Yang, X. Guan, and X. Cui, Engineering quantum magnetism in one-dimensional trapped Fermi gases with *p*-wave interactions, Phys. Rev. A **93**, 051605(R) (2016).

[44] X. Y. Yin, T.-L. Ho, and X. Cui, Majorana edge state in a number-conserving Fermi gas with tunable p-wave interaction, New J. Phys. **21**, 013004 (2019).

[45] H. Tajima, S. Tsutsui, T. M. Doi, and K. Iida, Unitary *p*-wave fermi gas in one dimension, Phys. Rev. A **104**, 023319 (2021).